N91-19193

GaAs Solar Cell Photoresponse Modeling Using PC-1D V2.1

D.A. Huber, L.C. Olsen, G. Dunham and F.W. Addis
Washington State University/Tri-Cities
Richland, WA

Introduction

In this study, photoresponse data of high efficiency GaAs solar cells have been analyzed using PC-1D V2.1. This paper discusses the approach required to use PC-1D for photoresponse data analysis, and the physical insights gained from performing the analysis. In particular, the effect of $Al_xGa_{(1-x)}As$ heteroface quality has been modeled. Photoresponse or spectral quantum efficiency is an important tool in characterizing material quality and predicting cell performance [ref. 1]. The strength of the photoresponse measurement lies in the ability to precisely fit the experimental data with a physical model. PC-1D provides a flexible platform for calculations based on these physical models.

Cell Fabrication and Performance

GaAs cell structures studied in this work were P/N homojunctions with $Al_xGa_{(1-x)}As$ heteroface layers for front and back minority carrier reflectors. All cells were 1.5 cm x 1.5 cm and fabricated from films grown on horizontal Bridgman wafers by MOCVD. The cells were fabricated from epi-structures supplied by SPIRE Corp., as well as grown in WSU/TC's SPI-MO CVD 500XT reactor. The SPIRE epitaxial layers were grown at atmospheric pressure using trimethylgallium, trimethylaluminum and 10% arsine in H_2. The WSU/TC cells were grown at low pressure using pure arsine. N-type doping was accomplished using silane and the p-type doping with dimethylzinc in H_2 in both cases. The basic structure described in Figure 1 was constant for these cells which facilitated side-by-side comparison of performance and material quality. Contacts for the devices were made by electroplating Au for the front contact and Au/Sn for the back contact. After sintering, the GaAs cap was removed between the contact fingers and a mesa was etched around the perimeter. The individual cells selected for this study correspond to varying growth conditions which affect the cell's performance [ref. 2]. These conditions include growth temperature of GaAs and $Al_xGa_{(1-x)}As$ as well as dopant flows and change of temperature at the heteroface. Efficiencies for these cells range from 18% to 22% for one-sun AM1.5 illumination. Cell performance is listed in Table 1.

Modeling Photoresponse Data with PC-1D V2.1

The Iowa State code PC-1D utilizes a finite element numerical approach to solve the semiconductor equations [ref. 3]. Version 2.1 allows significant improvements in the complexity of the problems that can be solved, compared to earlier versions [ref. 4]. Several key additions have proven especially applicable to the modeling of GaAs solar cells. The program permits modeling of minority carrier confinement due to the $Al_xGa_{(1-x)}As$ heteroface with recombination at the interface. PC-1D is equipped with an internal model for the absorption of $Al_xGa_{(1-x)}As$ as a function of x and permits the use of an external model or absorption data. Up to three regions of different material parameters can be used to define the device, each with its own doping profiles and electronic and optical properties. The ability to model the grading of material properties at the interface between each region increases the usefulness of the program to model realistic structures. Recombination of the electron hole pairs can be defined in each region by S-R-H band to band transitions or through user-defined deep level transitions. The recombination model can also account for Auger recombination, surface recombination at the interfaces within the device or saturation current terms.

The first approach at modeling heteroface GaAs solar cells divided the device into two materials an $Al_xGa_{(1-x)}As$ region in front of the GaAs homojunction region. The grading between these two materials was set at the minimum value of 10 Å, an abrupt interface. This generated photoresponse which was independent of surface recombination due to the high drift fields produced. Reasonable values for the grading thickness always led to the same result since the ΔE_G is large. The response of the cells, however, showed definite signs of front surface recombination. Incorporating our previously reported "dead layer" model allowed for an additional interface and recombination current [ref. 2].

For the cells studied, modeling studies with PC-1D predict the necessity of a thin defective GaAs region located between the emitter and the front $Al_xGa_{(1-x)}As$ layer where defect states result in current loss due to recombination within the region. This approach models the $Al_xGa_{(1-x)}As$ window region, a two-region emitter consisting of the defective layer and a high quality region, and an n-type base region. This is accomplished using three material parameter files - a wide bandgap $Al_xGa_{(1-x)}As$ material, a defective low-lifetime GaAs material, and a high quality GaAs material. Figure 2 shows a bandgap diagram illustrating the modeled regions. The effect of the back $Al_xGa_{(1-x)}As$ reflector was modeled only by a surface recombination velocity in this study since absorption of photons is inconsequential. This allows more flexiblity in the modeling of the front interface .

Results and Discussion

The model was used to produce a very close fit to the unique photoresponse of several cells. Figures 3 through Figure 7 show the experimental data for several cells as well as the modeled curves for comparison. The values modeled for individual cells are given in Table 2. The defective region size increases with $Al_xGa_{(1-x)}As$ growth temperature, which correlated with the length of transition time between GaAs growth and $Al_xGa_{(1-x)}As$ growth. Defective layer thickness varied from less than 30 Å to greater than 100 Å. Front surface recombination velocities ranged from 1×10^4 cm/s to approximately 2×10^5 cm/s. As shown previously, both a surface recombination and a finite "dead layer" thickness are needed to fit some devices due to the absorption in the thin defective region [ref. 4]. The modeled structures corresponded well with the layer thicknesses derived from electrochemical C-V profiling. Earlier cells could only be modeled using window Al concentrations lower than the $Al_{0.85}Ga_{0.15}As$ specified. $Al_xGa_{(1-x)}As$ concentrations were confirmed using surface photovoltage measurements and reflectance modeling. This was remedied in later growth runs which produced higher response. The internal model for photon absorption in $Al_xGa_{(1-x)}As$ included in PC-1D gives good magnitudes for the absorption coefficients but produces a rather jagged appearing curve compared with the smooth experimental curves. Our previous model based on Mazier's approach [ref. 5] and reported elsewhere gave somewhat lower but smoother coefficients [ref. 6].

Both defect layer thickness and surface recombination velocity were functions of growth conditions. Table 3 lists growth conditions for some of the cells studied. These studies lead to the conclusion that interrupted growth for a change of $Al_xGa_{(1-x)}As$ composition or temperature leads to the introduction of defect states which allow recombination in the vicinity of the heteroface. The cells grown at WSU/TC incorporated the results of the studies on earlier cells which produced devices with high internal photoresponse.

Acknowledgement

The authors wish to thank the Air Force Office of Scientific Research for support to investigate solar cells based on III-V compounds under Grant AFOSR-89-0182.

References

[1.] L. C. Olsen, et al., *Space Photovoltaic Research and Technology Conference*, NASA (1986).

[2.] L. C. Olsen, et al., *Proceedings of the Nineteenth IEEE Photovoltaic Specialists Conf.* (1987).

[3.] P. A. Basore, et al., *Proceedings of the Eighteenth IEEE Photovoltaic Specialists Conf.* (1988).

[4.] P. A. Basore, et al., *Proceedings of the Twentieth IEEE Photovoltaic Specialists Conf.* (1988).

[5.] C. Maziar, Subcontract Report - SERI/STR-211-2512, DE 85000501 (1984).

[6.] L. C. Olsen, et al., *Space Photovoltaic Research and Technology Conference*, NASA (1988).

TABLE 1
AM1.5 EFFICIENCIES

Cell	V_{oc} (V)	J_{sc} mA/cm^2	Fill Factor	Efficiency (%)
1	.954	22.6	.803	17.3
2	1.02	23.2	.82	19.3
3	1.02	24.91	.851	21.5
4	NA	22.1*	NA	NA
5	NA	25.4*	NA	NA

* Active Area Before Antireflection Layer

TABLE 2
MODELED PARAMETERS

Cell	S(F) cm/s	L(E) microns	L(B) microns	S(B) cm/s	X(DL) Å	X(WH) Å	Al (conc) %
1	2×10^5	3.0	2.0	1×10^4	100	500	65
2	2×10^4	5.0	0.2	1×10^7	50	500	70
3	1×10^4	5.0	4.0	1×10^4	30	500	75
4	1×10^4	>6.0	3.0	1×10^4	0	500	80
5	1×10^4	>6.0	4.0	1×10^4	0	500	80

TABLE 3
GROWTH PARAMETERS

Cell	NA(E) cm^{-3}	T(E) °C	T(BR) °C	ND(B) cm^{-3}	T(BASE) °C	T(AlGaAs) °C	X(AlGaAs) %
1	1×10^{18}	700	800	1×10^{17}	650	800	65
2	1×10^{18}	700	750	1×10^{18}	750	700	70
3	1×10^{18}	700	750	3×10^{17}	700	750	75
4 LP	1×10^{18}	720	720	1×10^{18}	720	720	80
5 LP	1×10^{18}	720	720	3×10^{17}	720	720	80

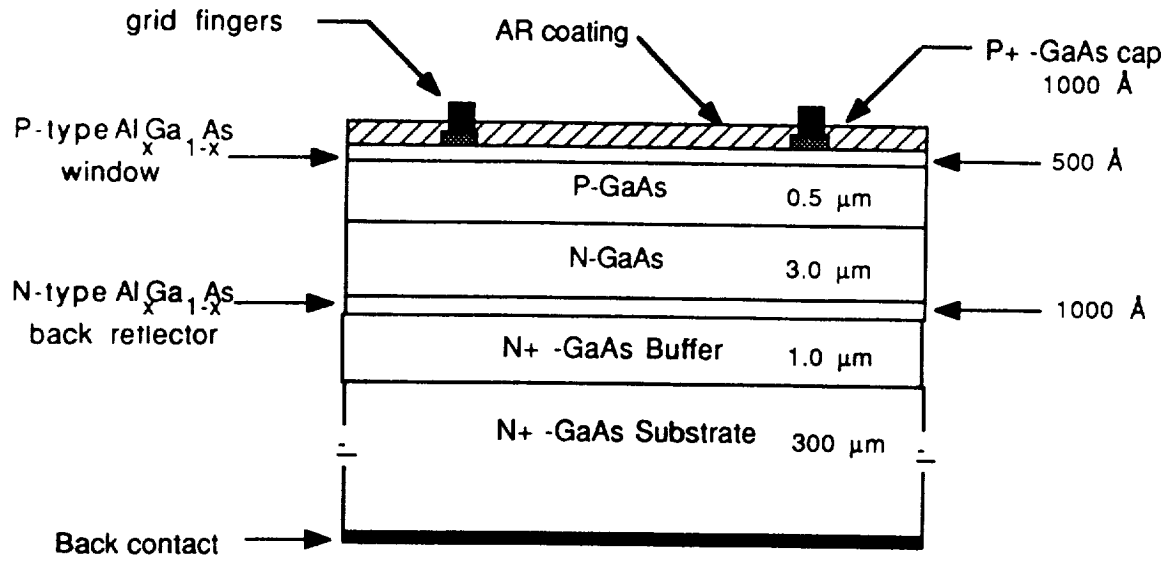

Figure 1 The basic structure for the high efficiency GaAs solar cells modeled.

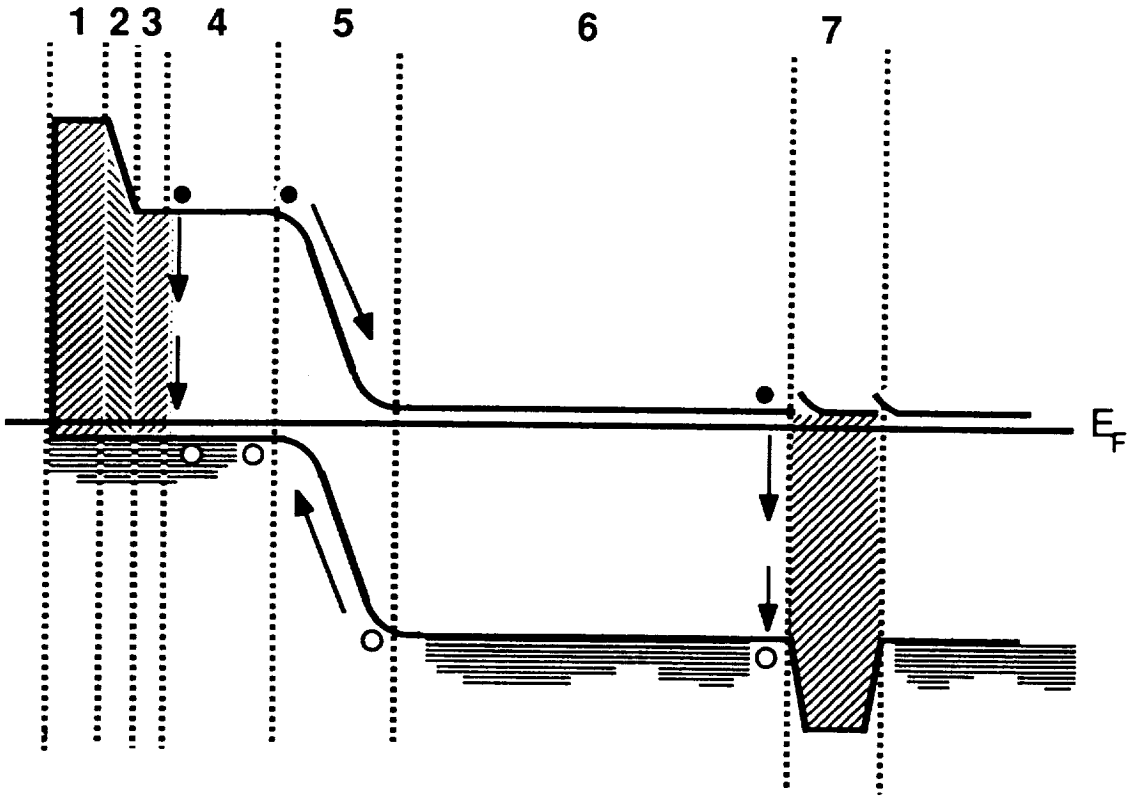

Figure 2 Energy bandgap diagram showing regions modeled using PC-1D.

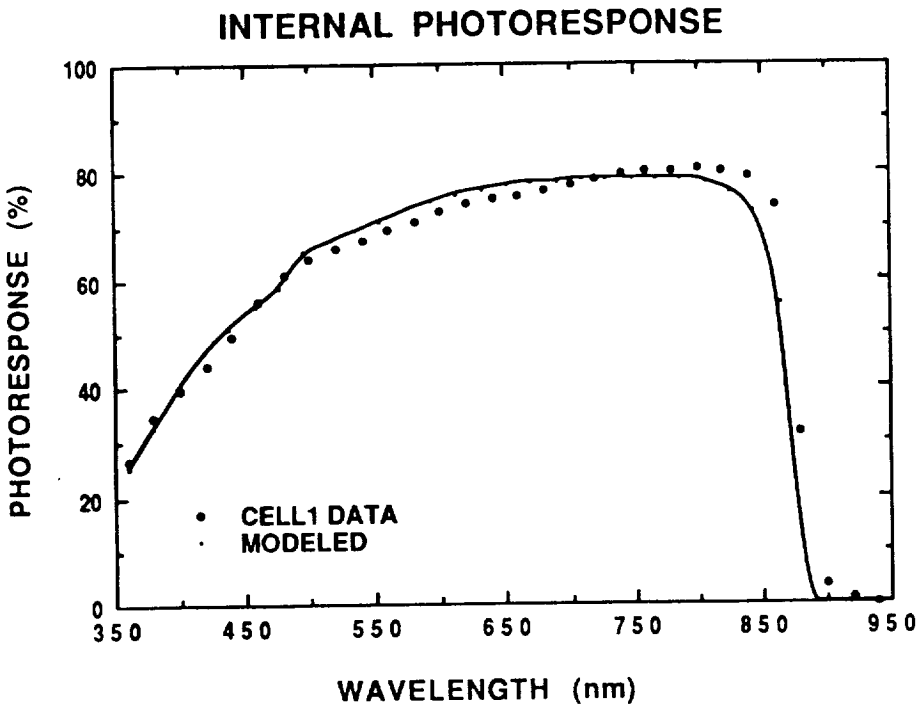

Figure 3 Photoresponse data and PC-1D model for CELL1

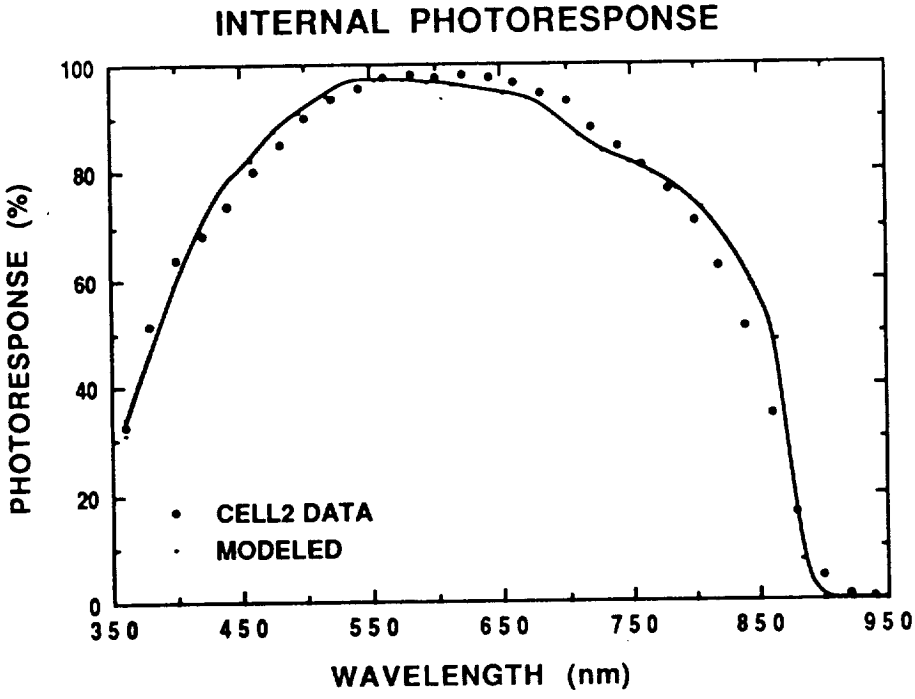

Figure 4 Photoresponse data and PC-1D model for CELL2

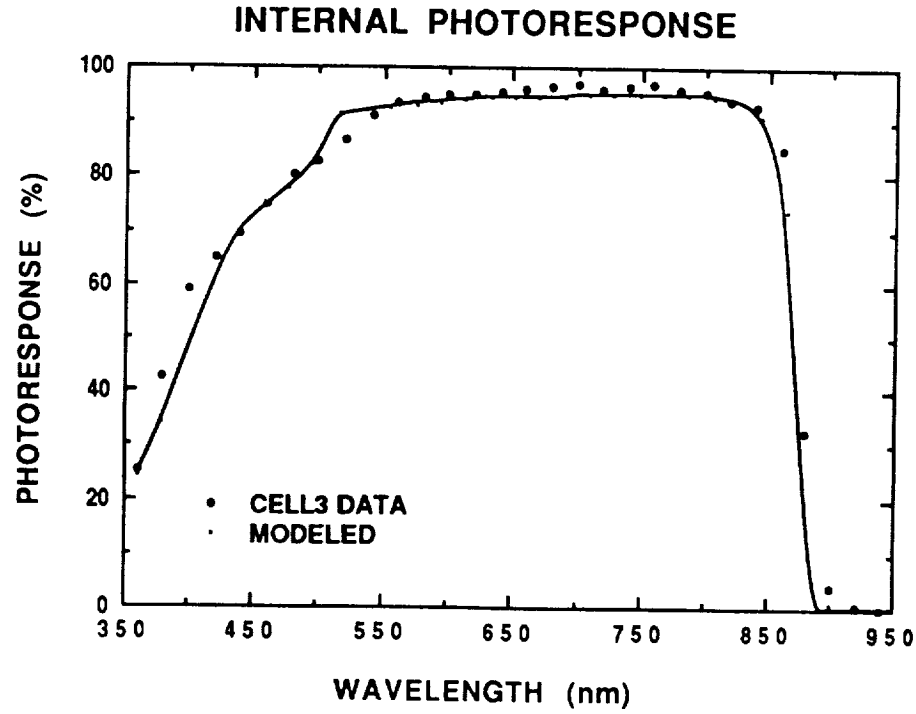

Figure 5 Photoresponse data and PC-1D model for CELL3

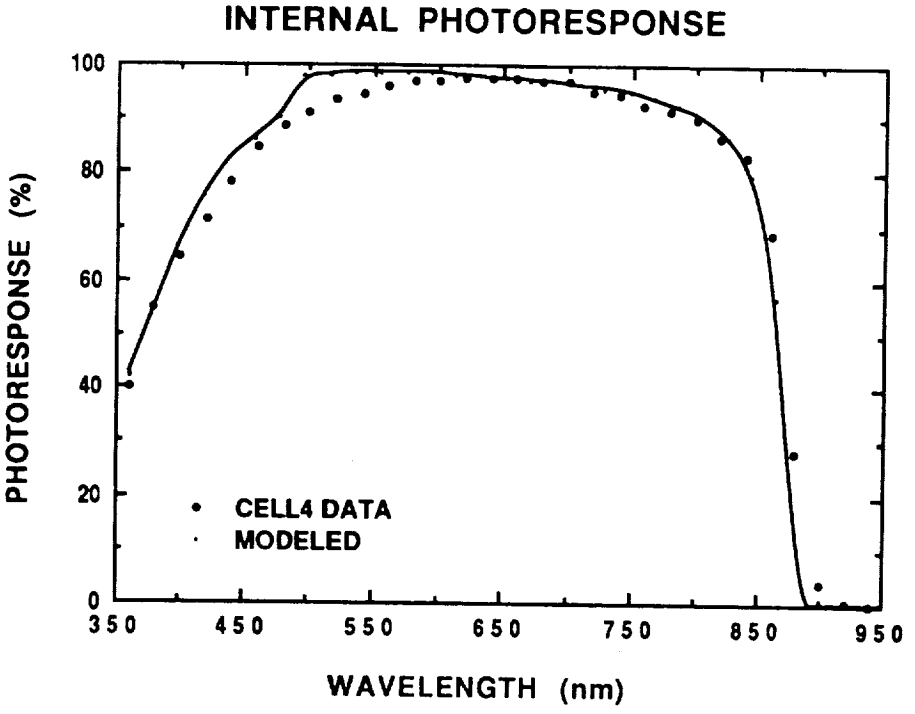

Figure 6 Photoresponse data and PC-1D model for CELL4

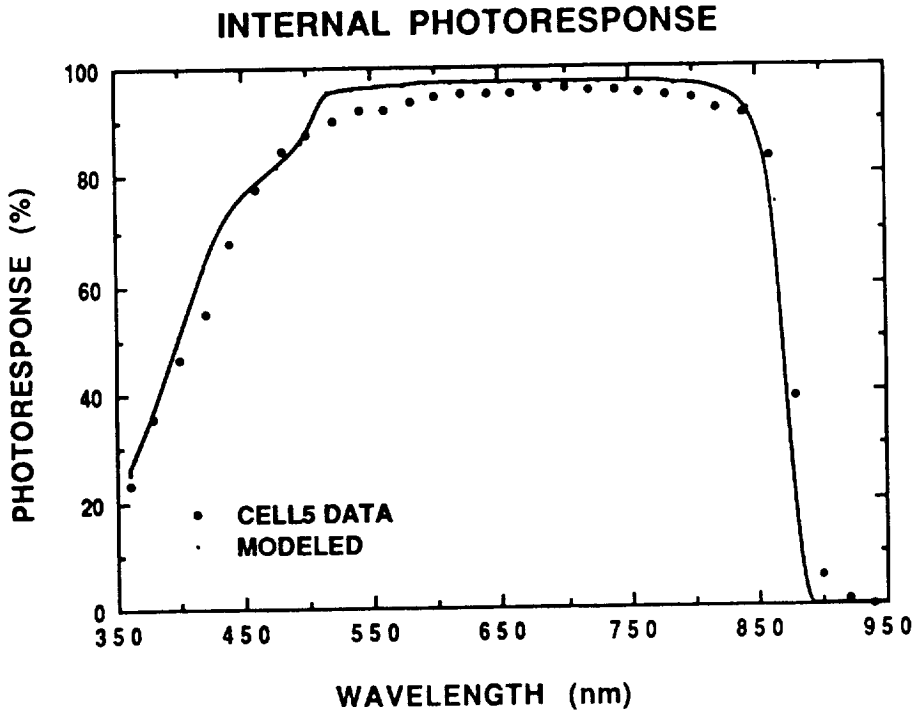

Figure 7 Photoresponse data and PC-1D model for CELL5